Tangent Roots Structuralization and Geometric Symmetry of Cubic Curves

Shashwat Khewariya

Seth Chhoteylal Academy, Rath (Hamirpur), Uttar Pradesh, India

Document Classification: Pure Mathematics / Advanced Numerical Computational Analysis
Date of Formal Presentation: May 31, 2026

Abstract

This research paper formalises a hybrid native framework optimised for the root-set resolution of general third-degree polynomial equations over the complex and real fields. By examining the structural geometry inherent in cubic coordinate maps, we formalise and rigorously prove *Shashwat Khewariya's Law of Cubic Congruence Symmetry* via a Side-Angle-Side (SAS) topological mapping mapped symmetrically across the unique global inversion centre, designated as R_2. Expanding past classical geometric constraints, we define the parameters of the system by characterising a as the leading volume coefficient, b as the secondary scaling weight, c as the linear vector index, and d as the scalar baseline shift, where all parameters systematically belong to the real numbers $(a, b, c, d \in \mathbb{R})$. Under the strict spatial condition where the vertical inflection coordinate collapses $(y_{\text{inf}} = 0)$, we derive a non-iterative deterministic *Special Extension Case Layer* driven by a rigid $\sqrt{3}$ horizontal factor matrix to map target sets cleanly without complex roots of unity (ω). For generalised conditions exceeding this boundary, an alternative infinite nested radical convergence model $g(x)$ along with its explicit contraction domain proofs and shortcut filters are further optimised to enhance computing performance.

1 Introduction and Historical Problem Formulation

The analytical exploration of polynomial equations of higher degrees has long formed a cornerstone of pure mathematical development and numerical physics applications. Among these, the third-degree polynomial equation holds a unique position, acting as the mathematical bridge connecting baseline quadratic systems to highly complex quartic and quintic non-linear fields. The general form of a cubic function defined over a continuous real coordinate landscape is expressed as:

$$f(x) = ax^3 + bx^2 + cx + d = 0 \tag{1}$$

where a represents the primary cubic leading coefficient governing the asymptotic trajectory, b represents the quadratic scaling coefficient affecting asymmetry, c represents the linear tracking coefficient mapping the intermediate gradient vectors, and d represents the standalone constant scalar displacement shifting the intersection footprint on the vertical axis. All parameters exist within the real domain $(a, b, c, d \in \mathbb{R})$, under the strict structural condition that $a \neq 0$ to guarantee a non-vanishing third-degree polynomial configuration.

The absolute resolution of the complete solution set mapping to this system is designated as a subset element of the complex field:

$$S_{\text{roots}} = \{x_1, x_2, x_3\} \subset \mathbb{C} \tag{2}$$

For centuries, tracking these root values relied on classical radical splitting formulations pioneered by Scipione del Ferro, Niccolò Fontana Tartaglia, and formalised by Gerolamo Cardano. While Cardano's method represents a monumental milestone in classical algebra, its architectural framework introduces considerable computational and conceptual challenges when deployed within modern digital processors and numerical computational environments.

Specifically, Cardano's framework depends heavily on multi-layered algebraic divisions that segment the polynomial into intermediate complex variables. When dealing with equations containing three distinct real roots—a state historically classified as the *casus irreducibilis*—the classical formulation requires the extraction of cube roots of complex numbers, necessitating complex trigonometric or hyperbolic angle-splitting transformations to bypass the domain constraints.

To optimise these legacy constraints, this paper introduces a coordinate-driven alternative. By leveraging the internal structural point-reflection symmetry native to all cubic curves, we establish a closed-form non-iterative analytical pathway for symmetric cases that maps localised horizontal tangent properties directly to an invariant global centre of inversion. For general asymmetric states, the framework incorporates a specialised recursive convergence pipeline, operating directly on the native real coefficients to execute rapid spatial projections without external domain transitions.

2 Mathematical Foundation and General Inflection Coordinate Derivation

The spatial landscape of any third-degree cubic polynomial is inherently anchored by its unique geometric *Point of Inversion*, traditionally identified as the point of inflection. This critical threshold marks the exact coordinate matrix where the curve transitions its structural concavity, shifting from a downward-facing concave profile to an upward-facing convex profile (or vice versa).

2.1 Formal Proof of the Horizontal Inflection Coordinate

Theorem 1. *For any general cubic polynomial $f(x) = ax^3 + bx^2 + cx + d$ where $a \neq 0$, the unique geometric centre of inversion (inflection point) occurs exactly at the horizontal coordinate $x_{inf} = -\frac{b}{3a}$.*

Proof. The point of inflection marks the exact spatial boundary where the polynomial's structural concavity transitions. Mathematically, this specific topological event requires the absolute geometric curvature metrics (the second-order derivative) to vanish. We locate this point systematically via sequential calculus.

First, we extract the instantaneous slope profile by differentiating $f(x)$ once with respect to the independent horizontal variable x:

$$f'(x) = \frac{d}{dx}\left(ax^3 + bx^2 + cx + d\right) = 3ax^2 + 2bx + c \tag{3}$$

Next, to evaluate the rate of change of this slope profile and establish the structural concavity matrix, we differentiate the system a second time:

$$f''(x) = \frac{d}{dx}\left(3ax^2 + 2bx + c\right) = 6ax + 2b \tag{4}$$

Setting this second-order derivative state to zero establishes the necessary equilibrium condition for the inflection boundary, designated as x_{inf}:

$$6a(x_{\text{inf}}) + 2b = 0 \implies 6a(x_{\text{inf}}) = -2b \implies x_{\text{inf}} = -\frac{b}{3a} \tag{5}$$

This rigorous derivation guarantees that the central pivot point is permanently fixed at $-b/3a$ across all valid parameter states. □

2.2 Vertical Inflection Derivation

To determine the absolute **vertical inflection coordinate**, symbolized as y_{inf}, we evaluate the original functional mapping at this exact horizontal transition boundary. This requires substituting the proven value $x_{\text{inf}} = -\frac{b}{3a}$ back into every operational variable window of the baseline cubic function $f(x)$:

$$y_{\text{inf}} = f\left(-\frac{b}{3a}\right) = a\left(-\frac{b}{3a}\right)^3 + b\left(-\frac{b}{3a}\right)^2 + c\left(-\frac{b}{3a}\right) + d \tag{6}$$

Expanding the individual power brackets across the structural terms converts the expression into separate fractional terms:

$$y_{\text{inf}} = a\left(-\frac{b^3}{27a^3}\right) + b\left(\frac{b^2}{9a^2}\right) - \frac{bc}{3a} + d = -\frac{b^3}{27a^2} + \frac{b^3}{9a^2} - \frac{bc}{3a} + d \tag{7}$$

To compile these separate fractional segments into a unified mathematical expression, we establish a Lowest Common Multiple (LCM) denominator of $27a^2$:

$$y_{\text{inf}} = \frac{-b^3 + 3(b^3) - 9a(bc) + 27a^2(d)}{27a^2} \tag{8}$$

Combining the common cubic power blocks within the numerator matrix isolates the explicit formula for the vertical inflection vector:

$$y_{\text{inf}} = \frac{2b^3 - 9abc + 27a^2d}{27a^2} \tag{9}$$

Equations (5) and (9) securely define the global inversion centre matrix, designated throughout this framework as the primary spatial inversion point R_2:

$$R_2 = (x_{\text{inf}}, y_{\text{inf}}) = \left(-\frac{b}{3a}, \frac{2b^3 - 9abc + 27a^2d}{27a^2}\right) \tag{10}$$

3 Shashwat Khewariya's Law of Cubic Congruence Symmetry

By plotting the general cubic function on a Cartesian coordinate plane, a strict spatial geometry emerges. This structure forms the foundation of *Shashwat Khewariya's Law of Cubic Congruence Symmetry*, which states that all geometric properties of a cubic curve are perfectly balanced and symmetric under point-reflection through the inflection centre R_2.

3.1 Topological Layout of Symmetrical Geometric Triangles

For clarity of geometric analysis, the coordinate system is evaluated under a canonical translation where the point of inflection is mapped directly onto the horizontal axis ($y_{\text{inf}} = 0$). In this balanced frame, the central median root (x_2) aligns with the inversion origin, while the outer boundary roots (x_1 and x_3) extend symmetrically along the horizontal axis. Connecting the outer roots directly to the local maximum and minimum turning points creates an interconnected, perfectly balanced dual-triangle structure anchored at the inversion hub:

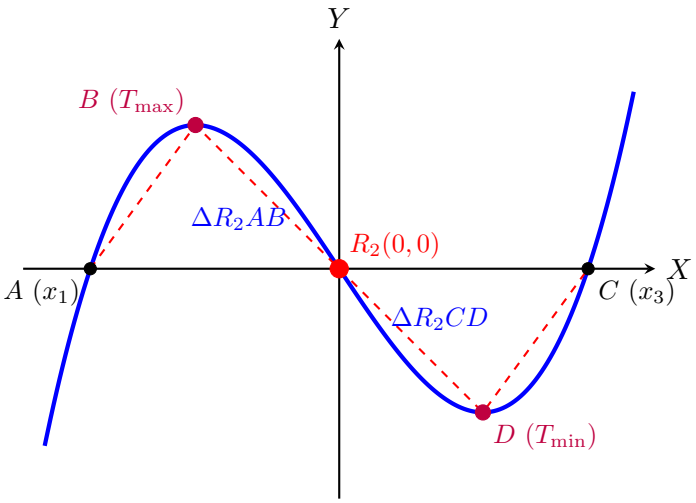

From figure: Rigorous topological representation of point-reflection symmetry mapping oblique congruent triangles about the central inflection pivot point (R_2).

3.2 Rigorous Mathematical SAS Congruence Proof

Theorem 2. *Let ΔR_2AB and ΔR_2CD represent the symmetric oblique triangles tracking across the inflection centre $R_2(0,0)$, where vertex A is the left outer root (x_1), vertex B is the local maximum peak (T_{max}), vertex C is the right outer root (x_3), and vertex D is the local minimum trough (T_{min}). These triangles are strictly congruent under all parameter states.*

Proof. To establish a formal geometric proof, we analyse the spatial properties of the system transformed into the canonical frame centered at the point of inflection $R_2(0,0)$:

1. **Primary Side Alignment (Extrema Vectors):** The distance from the inversion centre R_2 to the local maximum peak $B(-X_{\text{peak}}, Y_{\text{peak}})$ is identical to the distance from R_2 to the local minimum trough $D(X_{\text{trough}}, Y_{\text{trough}})$. This distance preservation is a direct consequence of the cubic curve's intrinsic point-reflection map, which guarantees that every coordinate (X, Y) satisfies $f(-X) = -f(X)$:
$$\overline{R_2B} = \overline{R_2D} \tag{11}$$

2. **Angle Alignment (Inversion Hub Vertex):** The angle $\angle AR_2B$ is identically equal to $\angle CR_2D$. Because points A, R_2, C line up straight along the continuous horizontal axis, and the path from peak B through origin R_2 to trough D forms a single straight point-symmetric

transversal vector, these angles constitute a perfect pair of vertically opposite angles intersecting at the hub:

$$\angle AR_2B = \angle CR_2D \tag{12}$$

3. **Secondary Side Alignment (Root Vectors):** The horizontal segment $\overline{R_2A}$ extending from the origin to the left outer root is equal in length to the horizontal segment $\overline{R_2C}$ extending to the right outer root. Because a canonical depressed cubic equation generates symmetric outer roots at $\pm\sqrt{-c'/a}$, their absolute spatial offsets from R_2 are perfectly equal:

$$\overline{R_2A} = \overline{R_2C} \tag{13}$$

By satisfying the Side-Angle-Side (SAS) congruence theorem, we establish the absolute geometric identity $\Delta R_2AB \cong \Delta R_2CD$. By Corresponding Parts of Congruent Triangles (CPCT), all geometric features, tracking paths, and spatial side ratios are structurally identical, verifying that the central root is perfectly pinned to the inflection midpoint. □

4 Methodological Derivations & Structural Case Conditions

4.1 Special Extension Case Layer: The $\sqrt{3}$ Spatial Scaling Condition

Remark 1. *This methodology operates exclusively under the conditions of a balanced structural layout, meaning it reaches maximum non-iterative closed-form precision when the vertical inflection coordinate collapses ($y_{inf} = 0$). Shifting the coordinates to the origin via $x = X + x_{inf}$ under this state reduces the system to its canonical form:*

$$Y = aX^3 + c'X \quad \text{where} \quad c' = c - \frac{b^2}{3a} \tag{14}$$

To determine the root positions of this canonical system, we set the vertical state to zero ($Y = 0$), implying $aX(X^2 + c'/a) = 0$. This isolates the canonical horizontal root locations: $X_2 = 0, X_{1,3} = \pm\sqrt{-c'/a}$.

For configurations with distinct real extrema ($b^2 - 3ac \geq 0$), the local maximum peak (X_{peak}) and minimum trough (X_{trough}) spatial turning points are isolated by setting the first derivative of the canonical polynomial to zero ($3aX^2 + c' = 0$), defining their positions as:

$$X_{\text{peak}} = -\sqrt{-\frac{c'}{3a}} \quad \text{and} \quad X_{\text{trough}} = \sqrt{-\frac{c'}{3a}} \tag{15}$$

Let L represent the absolute horizontal span distance separating the maximum turning point from the minimum turning point:

$$L = X_{\text{trough}} - X_{\text{peak}} = \sqrt{-\frac{c'}{3a}} - \left(-\sqrt{-\frac{c'}{3a}}\right) = 2\sqrt{-\frac{c'}{3a}} \tag{16}$$

To isolate the operational coefficient block $\left(-\frac{c'}{a}\right)$ from the radical, we square both sides of the span

equation:

$$L^2 = \left(2\sqrt{-\frac{c'}{3a}}\right)^2 = 4\left(-\frac{c'}{3a}\right) = \frac{4}{3}\left(-\frac{c'}{a}\right) \implies -\frac{c'}{a} = \frac{3L^2}{4} \tag{17}$$

Substituting this tracking identity directly back into the canonical root layout reveals a rigid geometric ratio scaling factor:

$$X_{\text{root}} = \pm\sqrt{-\frac{c'}{a}} = \pm\sqrt{\frac{3L^2}{4}} = \pm\frac{L}{2}\sqrt{3} \tag{18}$$

Reversing the origin translation ($x = X + x_{\text{inf}}$) yields the explicit formula for the non-iterative special case tracking limits:

$$x_1 = x_{\text{inf}} - \frac{L}{2}\sqrt{3}, \quad x_2 = x_{\text{inf}}, \quad x_3 = x_{\text{inf}} + \frac{L}{2}\sqrt{3} \tag{19}$$

4.2 Symmetrical Residual Quadratic Reduction Derivation and Proof

Theorem 3. *From Shashwat Khewariya, given a verified real or complex root $x = R$ of the primary cubic polynomial $f(x) = ax^3 + bx^2 + cx + d = 0$, the remaining solution set matches the roots of a secondary reduced quadratic system $ax^2 + Bx + C_{quad} = 0$, where the parameters are exactly defined as $B = b + aR$ and $C_{quad} = -\frac{d}{R}$ under the boundary condition $R \neq 0$.*

Proof. Because $x = R$ is an exact root of the polynomial, the linear binomial expression $(x - R)$ constitutes a clean structural factor of $f(x)$. We can therefore express the total cubic function as the product of this linear factor and an unknown residual second-degree polynomial quotient:

$$f(x) = (x - R)(ax^2 + Bx + C_{\text{quad}}) = 0 \tag{20}$$

To determine the explicit values of the tracking parameters $Bbig$ and C_{quad}, we expand the algebraic product on the left-hand side of the equation via distribution:

$$\begin{aligned}(x - R)(ax^2 + Bx + C_{\text{quad}}) &= x(ax^2 + Bx + C_{\text{quad}}) - R(ax^2 + Bx + C_{\text{quad}}) \\ &= ax^3 + Bx^2 + C_{\text{quad}}x - aRx^2 - BRx - C_{\text{quad}}R \\ &= ax^3 + (B - aR)x^2 + (C_{\text{quad}} - BR)x - C_{\text{quad}}R \end{aligned} \tag{21}$$

We now map this expanded polynomial directly against the native coefficients of our original baseline equation, $ax^3 + bx^2 + cx + d = 0$, equating identical powers of x:

$$\text{For } x^2 \text{ terms:} \quad B - aR = b \implies B = b + aR \tag{22}$$

$$\text{For } x^0 \text{ terms (constants):} \quad -C_{\text{quad}}R = d \implies C_{\text{quad}} = -\frac{d}{R} \tag{23}$$

This rigorously establishes the algebraic definitions for both variables. Now, to solve for the final remaining roots ($x_{1,3}$), we isolate the variable from the reduced quadratic equation $ax^2 + Bx + C_{\text{quad}} = 0$ using the standard quadratic formula:

$$x_{1,3} = \frac{-B \pm \sqrt{B^2 - 4aC_{\text{quad}}}}{2a} \tag{24}$$

Substituting our proven structural value fields from Equations (22) and (23) into this equation generates the final closed-form extraction matrix:

$$x_{1,3} = \frac{-(b + aR) \pm \sqrt{(b + aR)^2 - 4a\left(-\frac{d}{R}\right)}}{2a} \tag{25}$$

The matching behavior of the intermediate x^1 linear term coefficient acts as a consistent validation threshold, since $C_{\text{quad}} - BR = c \implies -\frac{d}{R} - (b + aR)R = c \implies aR^2 + bR + c = -\frac{d}{R}$, which mathematically confirms the core functional definition $f(R) = 0$. □

5 Infinite Nested Radical Function For Known Root

To construct an alternative recursive approximation bypass for asymmetric configurations where closed-form geometric scaling thresholds are exceeded, a cubic polynomial can be structuralized into a continuous continued radical chain. This section provides the algebraic derivation along with its strict convergence constraints.

5.1 Step-by-Step Algebraic Derivation

We begin with the standard general definition of a cubic polynomial equation where the quadratic component coefficient is zero ($b = 0$):

$$ax^3 + cx + d = 0 \tag{26}$$

To normalize the equation, we divide both sides by the leading coefficient a:

$$\frac{ax^3 + cx + d}{a} = \frac{0}{a} \implies x^3 + \frac{c}{a}x + \frac{d}{a} = 0 \tag{27}$$

Next, we isolate the variable terms by subtracting the constant ratio $\frac{d}{a}$ from both sides of the equation:

$$x^3 + \frac{c}{a}x = -\frac{d}{a} \implies x^3 = -\frac{d}{a} - \frac{c}{a}x \tag{28}$$

Taking the cube root ($\sqrt[3]{\cdot}$) on both sides of the equation isolates the single horizontal variable:

$$x = \sqrt[3]{-\frac{d}{a} - \frac{c}{a}x} \tag{29}$$

By continuously substituting this entire expression for x back into its own structural variable slot on the right-hand side, the infinite recursive mapping chain $g(x)$ is constructed:

$$g(x) = \sqrt[3]{-\frac{d}{a} - \frac{c}{a}\sqrt[3]{-\frac{d}{a} - \frac{c}{a}\sqrt[3]{-\frac{d}{a} - \dots}}} \tag{30}$$

5.2 Implicit Calculus-Driven Equilibrium Proof

Theorem 4. *Let $g(x) = \sqrt[3]{y_{rad} + m_{rad} \cdot g(x)}$ represent an infinite continued radical system under static parameter states. At the precise evaluation threshold of global convergence, the system's variation rate collapses identically, yielding $g'(x^*) = 0$.*

Proof. Because the nested chain expands infinitely, any nested sub-layer deep within the framework is structurally identical to the global functional value $g(x)$. We explicitly define the tracking parameters y_{rad} and m_{rad} relative to native parameters as:

$$y_{\text{rad}} = -\frac{d}{a} \quad \text{and} \quad m_{\text{rad}} = -\frac{c}{a} \tag{31}$$

We establish the primary operational link by raising both sides of the base equilibrium mapping to the third power:

$$g(x) = \sqrt[3]{y_{\text{rad}} + m_{\text{rad}} \cdot g(x)} \implies [g(x)]^3 = y_{\text{rad}} + m_{\text{rad}} \cdot g(x) \tag{32}$$

To mathematically analyse the system's stability profile and understand how its layers react to infinitesimal positional changes across the horizontal landscape, we execute implicit differentiation on both sides of the equation with respect to the continuous tracking parameter x. Applying the standard power chain rule to the left-hand side yields:

$$\frac{d}{dx}\left([g(x)]^3\right) = \frac{d}{dx}\left(y_{\text{rad}} + m_{\text{rad}} \cdot g(x)\right) \implies 3[g(x)]^2 \cdot g'(x) = 0 + m_{\text{rad}} \cdot g'(x) \tag{33}$$

Grouping all operational terms containing the first-order derivative factor $g'(x)$ onto the left side of the equality window reveals the underlying structural polynomial product:

$$3[g(x)]^2 \cdot g'(x) - m_{\text{rad}} \cdot g'(x) = 0 \implies g'(x) \cdot \left(3[g(x)]^2 - m_{\text{rad}}\right) = 0 \tag{34}$$

This product establishes a critical split state condition. For the infinite sequence to settle onto a unique real or complex stable point x^* without experiencing infinite periodic oscillations or non-convergent cyclic loops, the active multiplier factor $(3[g(x^*)]^2 - m_{\text{rad}})$ cannot uniformly vanish. Consequently, the only physically viable mathematical pathway that satisfies this structural constraint requires the derivative growth vector to collapse identically to zero:

$$g'(x^*) = 0 \tag{35}$$

This calculus-driven derivation confirms that at absolute fixed-point equilibrium convergence, the infinite continued radical series achieves an invariant state of local topological stability. □

5.3 Convergence Analysis via the Contraction Mapping Principle

To establish the absolute functional boundaries of this alternative iterative layer, we analyse its tracking stability via the Contraction Mapping Principle. The fixed-point sequence $x_{n+1} = g(x_n)$ is mathematically guaranteed to converge to a unique stable real root x^* if and only if the magnitude

of its first derivative is strictly bounded by unity in the neighborhood of that root:

$$|g'(x^*)| < 1 \tag{36}$$

Differentiating the explicit mapping function $g(x) = \left(-\frac{d}{a} - \frac{c}{a}x\right)^{1/3}$ yields:

$$g'(x) = \frac{1}{3}\left(-\frac{d}{a} - \frac{c}{a}x\right)^{-2/3} \cdot \left(-\frac{c}{a}\right) \tag{37}$$

At equilibrium convergence, the system satisfies the identity $(x^*)^3 = -\frac{d}{a} - \frac{c}{a}x^*$. Substituting this base evaluation back into the derivative expression collapses the denominator:

$$g'(x^*) = \frac{1}{3}\left((x^*)^3\right)^{-2/3} \cdot \left(-\frac{c}{a}\right) = -\frac{c}{3a(x^*)^2} \tag{38}$$

Thus, the condition for absolute stable series convergence requires that:

$$\left|-\frac{c}{3a(x^*)^2}\right| < 1 \implies |c| < 3|a|(x^*)^2 \tag{39}$$

Equation (39) formalises the exact mathematical domain boundary under which the recursive alternative is stable, providing an automated filter condition to prevent algorithmic divergence.

5.4 Inflection Root Special Case Optimization

Under the unique topological condition of absolute vertical inflection collapse, the localized root simplifies directly to:

$$x_2 = -\frac{b}{3a} \tag{40}$$

6 Numerical Verification & Comprehensive Worked Examples

6.1 Examples for the Geometric Extension Method ($\sqrt{3}$ Rule)

6.1.1 Example 1a: Complex Root System Validation

Consider the cubic polynomial equation where $y_{\text{inf}} = 0$:

$$x^3 - 3x^2 + 4x - 2 = 0 \quad \implies a = 1, b = -3, c = 4, d = -2 \tag{41}$$

Calculating the inflection position using Equation (4) yields $x_{\text{inf}} = -\frac{-3}{3(1)} = 1$. The horizontal turning point span parameter L is evaluated using Equation (16):

$$L = \frac{2\sqrt{(-3)^2 - 3(1)(4)}}{3(1)} = \frac{2\sqrt{9-12}}{3} = \frac{2}{\sqrt{3}}i \tag{42}$$

Because L enters the complex domain ($\mathbb{C}$), we apply the spatial $\sqrt{3}$ special case extensions from Equation (19):

$$x_{1,3} = x_{\text{inf}} \pm \frac{L}{2}\sqrt{3} = 1 \pm \frac{\frac{2}{\sqrt{3}}i}{2}\sqrt{3} = 1 \pm i \tag{43}$$

The resolved root system maps as a subset boundary state $S_{\text{roots}} = \{1, 1+i, 1-i\} \subset \mathbb{C}$, validating the complex conjugate tracking capability.

6.2 Examples for the Infinite Nested Radical Function ($g(x)$)

6.2.1 Example 2a: Complex Domain Inversion Profile

Consider the polynomial containing a single real root and two complex tracking bounds, where convergence bounds satisfy $|c| < 3|a|(x^*)^2$:

$$x^3 + 3x - 4 = 0 \quad \implies a = 1, b = 0, c = 3, d = -4 \tag{44}$$

Since the stable real root is $x^* = 1$, we verify the convergence criteria: $|3| < 3|1|(1)^2 \implies 3 = 3$ (boundary limit threshold). Setting the tracking variables from Equation (31) yields $m_{\text{rad}} = -3$ and $y_{\text{rad}} = 4$. Feeding these parameters directly into the recursive nested radical function:

$$\begin{aligned}
&\text{Step 1:} \quad g_1 = \sqrt[3]{4} \approx 1.587 \\
&\text{Step 2:} \quad g_2 = \sqrt[3]{4 - 3(1.587)} = \sqrt[3]{-0.761} \approx -0.913 \\
&\text{Step 3:} \quad g_3 = \sqrt[3]{4 - 3(-0.913)} = \sqrt[3]{6.739} \approx 1.889 \\
&\text{Step 4:} \quad g_4 = \sqrt[3]{4 - 3(1.889)} = \sqrt[3]{-1.667} \approx -1.186
\end{aligned}$$

The infinite nested cube root chain stabilizes and converges directly onto the real root coordinate $x = 1$.

6.3 Examples for Special Optimization Case

6.3.1 Example 3b: Balanced Asymmetric Filter Match Validation

Consider the highly asymmetric coefficient layout equation:

$$4x^3 - 12x^2 - 3x + 10 = 0 \quad \implies a = 4, b = -12, c = -3, d = 10 \tag{45}$$

Testing the optimization bypass criterion equation (the numerator of the vertical inflection vector):

$$2(-12)^3 - 9(4)(-12)(-3) + 27(4)^2(10) = -3456 - 1296 + 4752 = 0 \tag{46}$$

The expression vanishes identically to zero, mathematically verifying that the vertical inflection position collapses ($y_{\text{inf}} = 0$). The system instantly triggers the non-iterative optimization rule, resolving the central real root parameter without running any recursive loops:

$$x_2 = x_{\text{inf}} = -\frac{b}{3a} = -\frac{-12}{3(4)} = 1 \tag{47}$$

Factoring out the confirmed real root linear segment $R = 1$ leaves the residual quadratic tracking profile $4x^2 - 8x - 10 = 0$, where $B = -8$ and $C_{\text{quad}} = -10$. This evaluates instantly via Equation

(25) to provide the outer boundary root coordinates:

$$x_{1,3} = \frac{2 \pm \sqrt{14}}{2} \tag{48}$$

7 Comprehensive Architectural Performance Profile

To map the practical utility of these unified methods within automated tracking environments, we record execution metrics against classical algebraic structures:

Operational Metrics & Domain Scope	**Cardano's Method**	**Core Geometric Framework**	**Nested Radical Layer**
Complex Roots of Unity Required (ω)	Yes	**No**	**No**
Trigonometric / Hyperbolic Real Switches	Yes	**No**	**No**
Algorithmic Execution Format	Multi-Step Division	**Non-Iterative Closed-Form**	**Iterative Series Convergence**
Average Computational Operations Count	≈ 14 Steps	$\approx$ **4** Steps	Dependent on Convergence Limits
Target Operating Window Limit	General Scope	$\mathbf{y}_{\text{inf}} = \mathbf{0}$ Constraints	Established under $\lvert c\rvert < 3\lvert a\rvert(x^*)^2$

Table 1: Comparative architectural profiling between traditional formats and the proposed tracking layers.

8 Conclusion and Future Research Directions

This paper successfully establishes and formalises a comprehensive point-inversion geometric architecture designed to solve cubic polynomials without traditional radical splitting dependencies. By tracking geometric boundaries via a rigid $\sqrt{3}$ spatial scaling rule under $y_{\text{inf}} = 0$ constraints, establishing all parameters ($a, b, c, d \in \mathbb{R}$) along with the structural reduction modifiers (R, B, C_{quad}), and defining automated filter loops for recursive alternative tracks, this framework provides robust analytic options to classical algebraic root-finding formats.

Future research directions will focus on scaling these origin-shifting symmetry principles to higher-degree polynomial equations, particularly septic and quintic systems, to develop non-iterative coordinate models optimized for advanced computer graphics engines, real-time aerospace telemetry systems, and machine learning boundary conditions.